



## Synthesis, Characterization and Microbicides Activities of N-(hydroxy-4-((4-nitrophenyl)diazanyl) benzylidene)-2-(phenylamino) Acetohydrazide Metal Complexes



Ahmed N. Al-Hakimi\*<sup>1,2</sup>

<sup>1</sup>Chemistry Department, College of Science, Qassim University, Saudi Arabia.

<sup>2</sup>Faculty of Science, Chemistry Department, Ibb University, Ibb, Yemen.

**V**O(II), Cu(II), Ni(II), Co(II), Mn(II), Fe(III), Ru(III), Zn(II) and UO<sub>2</sub>(II) complexes of hydrazone ligand containing azo group as side chain were prepared from condensation of 2-hydroxy-4-((4-nitrophenyl)diazanyl) benzylidene)benzaldehyde with 2-(phenyl amino) acetohydrazide. The ligand and its complexes were isolated in solid state and characterized by analytical techniques such as elemental analyses, molar conductance, magnetic susceptibility measurements and Electronic spin resonance (ESR) as well as spectroscopic techniques such as UV-Visible, IR, <sup>1</sup>H-NMR and <sup>13</sup>C-NMR. The spectral data indicated that the ligand acted as neutral bidentate or monobasic tridentate ligand bonded to the metal ions through an oxygen atom of ketonic or enolic carbonyl group, an azomethine nitrogen atom and deprotonated phenolic oxygen atom forming either tetragonally distorted octahedral or square planer geometry. ESR spectra of the solid metal complexes (**2-6**) and (**8**) were studied. Antimicrobial activities of the ligand and its complexes were evaluated against *E. coli*, *Bacillus subtilis* and *Aspergillus Niger* by well diffusion method. Results showed that the complex (**10**) exhibited higher antifungal activity, complex (**7**) exhibited higher antibacterial than the other complexes against *E. coli*, while complex (**10**) exhibited higher antibacterial against *B.subtilis* than the other complexes.

**Keywords:** Azohydrazone, acetohydrazide, metal complexes, bioactivity, ESR

### Introduction

Hydrazone compounds are a category of Schiff base compounds with N-N linkage. Schiff base is compound showed widely spread because of their high effectiveness. These compounds were drawn a significant interest to medicinal chemical researchers for several years because of its varied biological and pharmaceutical implementations. For example, enzymatic activity antifertility, antimicrobial, antitumor, antiviral, anti-inflammatory, allergic inhibitors reducing activity radical scavenging [1-5]. The activity of these compounds due to the presence of the azomethine group and other subunits groups surrounding the azomethine group. Moreover, Hydrazones and their transition metal complexes are intensively studied in connection with the increasing use of them as pharmaceuticals, analytical reagents, and pesticides. Particularly highly interest the researchers paid to

the heterocyclic derivatives of hydrazine, the corresponding hydrazones, and complexes based on them, because of their biological activities[6-10]. Metal elements play an important role in increasing the effectiveness of Schiff base compounds because of their reception of the electrons as well as the charges it carries. On the other hand, azo compounds are the largest class of industrial synthesized organic dyes and have versatile applications in various fields. In recent years the study of azo dyes and their metal complexes has been of much interest because of their application in various fields such as dyes, redox indicators, and metallochromic reagents, biomedical studies, Potential drugs, and high technology areas such as laser and electro-optical devices. Azo compounds have also played an essential role as antibacterial, antifungal, anticancer, antituberculosis agents. Azo Schiff base complexes have the most im-

\*Corresponding author E-mail: [Alhakemi10@yahoo.com](mailto:Alhakemi10@yahoo.com), [anmalhakimi@yahoo.com](mailto:anmalhakimi@yahoo.com). Tel. 00966592550906

Received 16/12/2019; Accepted 04/02/2020

DOI: 10.21608/ejchem.2020.20906.2256

©2020 National Information and Documentation Center (NIDOC)

portant stereochemical models in coordination chemistry due to their preparative accessibility and structural variety.[11-15]. From this point of view, this work aims to synthesize, characterize, and evaluate antibacterial and antifungal activities of diverse azo-containing (2-hydroxy-4-((4-nitrophenyl) diazenyl) benzaldehyde) and hydrazide containing 2-(phenylamino)acetohydrazide.

## Experimental

### Chemicals and Instruments

All reagents employed for the preparation of the ligands and their complexes were of the analytical grade and used without further purification. 2-hydroxy-4-((4-nitrophenyl) diazenyl) benzaldehyde and 2-(phenylamino)acetohydrazide were prepared by published methods [16,17]. DMSO (assay 99.7%) and absolute ethanol (assay  $\geq$  99.8 %) were used. Metal salts:  $\text{Cu}(\text{CH}_3\text{COO})_2 \cdot \text{H}_2\text{O}$ ,  $\text{CuCl}_2 \cdot 2\text{H}_2\text{O}$ ,  $\text{Cu}(\text{NO}_3)_2 \cdot 2.5\text{H}_2\text{O}$ ,  $\text{Cu}(\text{SO}_4) \cdot 5\text{H}_2\text{O}$ ,  $\text{Ni}(\text{CH}_3\text{COO})_2 \cdot 4\text{H}_2\text{O}$ ,  $\text{Co}(\text{CH}_3\text{COO})_2 \cdot 4\text{H}_2\text{O}$ ,  $\text{Mn}(\text{CH}_3\text{COO})_2 \cdot 4\text{H}_2\text{O}$ ,  $\text{Zn}(\text{CH}_3\text{COO})_2 \cdot 2\text{H}_2\text{O}$ ,  $\text{FeCl}_3 \cdot 6\text{H}_2\text{O}$  were provided from SIGMA-ALDRICH company with purity ranged from 98 % to 99.995%.  $\text{UO}_2(\text{CH}_3\text{COO})_2 \cdot 2\text{H}_2\text{O}$  (assay  $\geq$  99.9 %),  $\text{UO}_2(\text{NO}_3)_2$  (assay  $\geq$  99.9 %),  $\text{VOSO}_4$  (assay  $\geq$  99.99 %),  $\text{RuCl}_3 \cdot 3\text{H}_2\text{O}$  (assay  $\geq$  99.9 %) were provided from American-Elements. TLC confirmed the purity of all prepared compounds. Elemental analysis (CHN) was performed in the Analytical Unit within Cairo University (Egypt) by the usual methods of analysis. Standard analytical methods were used to determine the metal ion content [18-20]. IR spectra of the solid ligand and complexes were recorded on a Perkin Elmer 681 and Perkin Elmer 1430 spectrometer as KBr pellets in the Analytical Unit within Cairo University (Egypt). The  $^1\text{H}$ - and  $^{13}\text{C}$ -NMR spectra were recorded with a JEOL JNM-ECP-400 MHz FT-NMR spectrometer in  $d_6$ -DMSO as a solvent, where the chemical shifts were determined relative to the solvent peaks. The ESR spectra of the solid complexes were recorded using a Varian E-4 spectrometer in 3-mm Pyrex tubes at 298 K. Diphenylpicryl hydrazide (DPPH) was used as a g-marker for the calibration of the spectra. The equation used to determine g-values is:

$$g = (g_{\text{DPPH}}) (H_{\text{DPPH}}) / H$$

Where:  $g_{\text{DPPH}} = 2.0036$

$H_{\text{DPPH}}$  = the magnetic field of DPPH in gauss

H = the magnetic field of the sample in gauss

The molar conductivity of the metal complexes

in DMSO at  $10^{-3}$  M concentration was measured using a dip cell and a Bibby conductimeter type MC1 at room temperature. The resistance measured in ohms and the molar conductivities were calculated according to the equation:

$$\Lambda_M = \frac{V \times K \times g}{Mw \times \Omega}$$

where:  $\Lambda$  = molar conductivity ( $\text{ohm}^{-1} \text{cm}^2 \text{mol}^{-1}$ ), V = volume of the complex solution, K = cell constant  $0.92 \text{cm}^{-1}$ , Mw = molecular weight of the complex, g = weight of the complex,  $\Omega$  = resistance measured in ohms. Electronic absorption spectra were recorded on UV-6100PCS double-beam spectrometer using 1cm quartz cells taking DMSO as the solvent. Magnetic susceptibilities were measured at  $25^\circ\text{C}$  by the Gouy method using mercuric tetrathiocyanatocobaltate(II) as the magnetic susceptibility standard. Diamagnetic corrections were estimated from Pascal's constant [21]. The magnetic moments were calculated from the equation:

$$\mu_{\text{eff}} = 2.84 \sqrt{\chi_M^{\text{corr}} \cdot T}$$

The thermal analyses (DTA and TGA) were carried out in the air on a Shimadzu DT-30 thermal analyzer from 27 to  $800^\circ\text{C}$  at a heating rate of  $10^\circ\text{C}$  per minute.

### Synthesis of ligand, N-(hydroxy-4-((4-nitrophenyl) diazenyl)benzylidene)-2-(phenylamino)acetohydrazide ( $H_3L$ ) (1)

2-hydroxy-4-((4-nitrophenyl) diazenyl) benzaldehyde (2.71 g, 0.01 mol, in 20 mL of absolute ethanol) was added to 2-(phenylamino)acetohydrazide (1.65 g, 0.01 mol, in 20 ml of absolute ethanol) [Fig. 1]. The mixture was refluxed while stirring for one hour. The formed solid product was filtered off, washed with cold ethanol, followed by crystallization from ethanol and finally dried under vacuum over anhydrous  $\text{CaCl}_2$ . (FW = 418.41), Yield: 85%, Color: Dark yellow. *Elemental Anal.* Calc.% C, 60.28; H, 4.34; N, 20.09. Found% C, 59.79; H, 4.18; N, 19.66. IR spectra of  $H_3L$ , (KBr,  $\text{cm}^{-1}$ ): 3409(br)  $\nu(\text{OH})$ ,  $\nu(\text{NH})$  3359, 3258, 3100, 1694  $\nu(\text{C}=\text{O})$ , 1607  $\nu(\text{C}=\text{N})$ , 1572, 1485  $\nu(\text{N}=\text{N})$ , 1257  $\nu(\text{C}-\text{O})$ , 970  $\nu(\text{N}-\text{N})$ .  $^1\text{H-NMR}$  ( $\text{DMSO}-d_6$ , 400 MHz):  $\delta = 5.2$  (s, 1H, OH), 7.85 (s, H, NH), 4.3 (s, 1H, Ph-NH), 8.10 (s, 1H, N=C-H), 6.43-8.19 ppm (m, 12 H, aromatic protons).  $^{13}\text{C-NMR}$  spectrum of  $H_3L$  ( $\text{DMSO}-d_6$ , 400 MHz):  $\delta = 173$  (C=O), 161.3 (C-OH), 150.2 (C=NH), 143.5 (C-NH), 111-139.1 (aromatic carbon).

*Preparation of the metal complexes*

Metal complexes; **(2)**, **(6)**, **(9-11)** and **(13)** were prepared by mixing a hot ethanoic solution of the metal salts:  $\text{VOSO}_4 \cdot \text{H}_2\text{O}$ ,  $\text{CuSO}_4 \cdot 5\text{H}_2\text{O}$ ,  $\text{Mn}(\text{CH}_3\text{COO})_2 \cdot 4\text{H}_2\text{O}$ ,  $\text{FeCl}_3 \cdot 6\text{H}_2\text{O}$ ,  $\text{RuCl}_3 \cdot 3\text{H}_2\text{O}$ , and  $\text{UO}_2(\text{CH}_3\text{COO})_2$  with a suitable amount of a hot ethanoic solution of the ligand in molar ratio 1M : 1 L (metal : ligand) in the presence of 2 mL of triethylamine (TEA) To precipitate. The reaction mixture was then refluxed for 3 hours. The formed precipitates were filtered off, washed with ethanol, then with diethyl ether and dried under vacuum over anhydrous  $\text{CaCl}_2$ . The same method is used to prepare complexes; **(3-5)**, **(7-8)** and **(12)** but in molar ratio 1M : 1L (metal : ligand) in absence triethylamine (TEA).

**Vanadyl(IV) complex (2)**,  $[\text{VO}(\text{H}_2\text{L})_2(\text{H}_2\text{O})] \text{C}_{42}\text{H}_{36}\text{N}_{12}\text{O}_{10}$  (FW = 919.77), Yield: 55%, M.P. >300. Color: light brown, Molar conductance ( $\Lambda$ ) is  $25.5 \Omega^{-1}\text{cm}^2\text{mol}^{-1}$ . *Elemental Anal.* Calcd.% C, 54.84; H, 3.95; N, 18.27; V, 5.54; Found% C, 53.99.; H, 3.89; N, 17.90; V, 5.32; IR (KBr,  $\text{cm}^{-1}$ ): 3423(br)  $\nu(\text{H}_2\text{O})$ , 3360, 3259, 3100  $\nu(\text{NH})$ , 1694  $\nu(\text{C}=\text{O})$ , 1609  $\nu(\text{C}=\text{N})$ , 1485  $\nu(\text{N}=\text{N})$ , 1270  $\nu(\text{C}-\text{O})_{\text{ph}}$ , 1033  $\nu(\text{N}-\text{N})$ , 561  $\nu(\text{M} \leftarrow \text{O})$ , 505  $\nu(\text{M} \leftarrow \text{N})$ .

**Copper(II) complex (3)**,  $[\text{Cu}(\text{H}_2\text{L})(\text{CH}_3\text{COO})]$ ,  $\text{C}_{23}\text{H}_{22}\text{CuN}_6\text{O}_6$  (FW = 540.00), Yield: 67%, Melting points (M.P.) >300. Color: brown, Molar conductance ( $\Lambda$ ) is  $13.3 \Omega^{-1}\text{cm}^2\text{mol}^{-1}$ . *Elemental Anal.* Calcd.% C, 51.16; H, 3.73; N, 15.56; Cu, 11.77; Found% C, 50.69.; H, 3.45; N, 15.25; Cu, 11.55; IR (KBr,  $\text{cm}^{-1}$ ): 3363, 3261, 3090  $\nu(\text{NH})$ , 1693  $\nu(\text{C}=\text{O})$ , 1605  $\nu(\text{C}=\text{N})$ , 1474  $\nu(\text{N}=\text{N})$ , 1277  $\nu(\text{C}-\text{O})_{\text{ph}}$ , 965  $\nu(\text{N}-\text{N})$ , 620  $\nu(\text{M} \leftarrow \text{O})$ , 499  $\nu(\text{M} \leftarrow \text{N})$ , 1522, 1338 ( $\Delta = 184$ )  $\nu_{\text{sym}} \text{CH}_3\text{COO}$ ,  $\nu_{\text{asym}} \text{CH}_3\text{COO}$ .

**Copper(II) complex (4)**,  $[\text{Cu}(\text{H}_2\text{L})\text{Cl}] \cdot \text{C}_{21}\text{H}_{17}\text{CuN}_6\text{O}_4\text{Cl}$  (FW = 516.40), Yield: 62%, M.P. >300. Color: green, Molar conductance ( $\Lambda$ ) is  $15.4 \Omega^{-1}\text{cm}^2\text{mol}^{-1}$ . *Elemental Anal.* Calcd.% C, 48.84; H, 3.32; N, 16.27; Cu, 12.31; Found: C, 48.68.; H, 3.08; N, 15.99; Cu, 12.25; IR spectra (KBr,  $\text{cm}^{-1}$ ): 3360, 3259, 3100  $\nu(\text{NH})$ , 1693  $\nu(\text{C}=\text{O})$ , 1605  $\nu(\text{C}=\text{N})$ , 1460  $\nu(\text{N}=\text{N})$ , 1277  $\nu(\text{C}-\text{O})_{\text{ph}}$ , 965  $\nu(\text{N}-\text{N})$ , 620  $\nu(\text{M} \leftarrow \text{O})$ , 499  $\nu(\text{M} \leftarrow \text{N})$ .

**Copper(II) complex (5)**,  $[\text{Cu}(\text{H}_2\text{L})(\text{NO}_3)(\text{H}_2\text{O})_3]$ ,  $\text{C}_{21}\text{H}_{21}\text{CuN}_7\text{O}_9$  (FW = 578.99), Yield% 55%, M.P. >300. Color: olive, Molar conductance ( $\Lambda$ ) is  $12.1 \Omega^{-1}\text{cm}^2\text{mol}^{-1}$ . *Elemental Anal.* Calcd.% C, 43.56; H, 3.66; N, 16.93; Cu, 10.98; Found: C, 43.52.; H, 3.92; N, 16.21; Cu, 10.59; IR spectra (KBr,  $\text{cm}^{-1}$ ): 3434(br)  $\nu(\text{H}_2\text{O}/\text{OH})$ , 3343, 3110, 1605  $\nu(\text{C}=\text{N})$ ,

1523  $\nu(\text{N}=\text{C}-\text{O})$ , 1465  $\nu(\text{N}=\text{N})$ , 1380  $\nu(\text{C}-\text{O})_{\text{ph}}$ , 1257  $\nu(\text{C}-\text{O})_{\text{ph}}$ , 1023  $\nu(\text{N}-\text{N})$ , 590  $\nu(\text{M}-\text{O})$ , 478  $\nu(\text{M} \leftarrow \text{N})$ , 1466, 1373 ( $\Delta = 93$ )  $\nu(\text{NO}_3)$ .

**Copper(II) complex (6)**,  $[\text{Cu}(\text{H}_3\text{L})_2(\text{SO}_4)(\text{H}_2\text{O})]$ ,  $\text{C}_{42}\text{H}_{40}\text{CuN}_{12}\text{O}_{13}\text{S}$  (FW = 1014.51), Yield% 61%, M.P. >300. Color: olive, Molar conductance ( $\Lambda$ ) is  $9.9 \Omega^{-1}\text{cm}^2\text{mol}^{-1}$ . *Elemental Anal.* Calcd.% C, 49.73; H, 3.78; N, 16.57; Cu, 6.26; Found% C, 50.60.; H, 3.49; N, 16.25; Cu, 5.89; IR spectra (KBr,  $\text{cm}^{-1}$ ): 3434(br)  $\nu(\text{H}_2\text{O}/\text{OH})$ , 3356, 3259, 3106 (NH), 1694  $\nu(\text{C}=\text{O})$ , 1605  $\nu(\text{C}=\text{N})$ , 1464  $\nu(\text{N}=\text{N})$ , 1288  $\nu(\text{C}-\text{O})_{\text{ph}}$ , 980  $\nu(\text{N}-\text{N})$ , 590  $\nu(\text{M} \leftarrow \text{O})$ , 467  $\nu(\text{M} \leftarrow \text{N})$ , 1193, 1023, 896  $\nu(\text{SO}_4)$ ,

**Nickel complex (7)**,  $[\text{Ni}(\text{HL})(\text{CH}_3\text{COO})(\text{H}_2\text{O})_2]$ ,  $\text{C}_{23}\text{H}_{23}\text{NiN}_6\text{O}_8$  (FW = 571.17), Yield: 67%, M.P. >300. Color: brown, Molar conductance ( $\Lambda$ ) is  $13.3 \Omega^{-1}\text{cm}^2\text{mol}^{-1}$ . *Elemental Anal.* Calcd.% C, 48.37; H, 4.24; N, 14.71; Ni, 10.28; Found % C, 48.80.; H, 4.42; N, 14.25; Ni, 10.21; IR (KBr,  $\text{cm}^{-1}$ ): 3421(br)  $\nu(\text{H}_2\text{O}/\text{OH})$ , 3272, 3101  $\nu(\text{NH})$ , 1604  $\nu(\text{C}=\text{N})$ , 1518  $\nu(\text{N}=\text{C}-\text{O})$ , 1465  $\nu(\text{N}=\text{N})$ , 1257  $\nu(\text{C}-\text{O})_{\text{ph}}$ , 1018  $\nu(\text{N}-\text{N})$ , 566  $\nu(\text{M}-\text{O})$ , 489  $\nu(\text{M} \leftarrow \text{N})$ , 1540, 1336 ( $\Delta = 204$ )  $\nu_{\text{sym}} \text{CH}_3\text{COO}$ ,  $\nu_{\text{asym}} \text{CH}_3\text{COO}$ .

**Cobalt(II) complex (8)**,  $[\text{Co}(\text{H}_2\text{L})(\text{CH}_3\text{COO})]$ ,  $\text{C}_{23}\text{H}_{20}\text{CoN}_6\text{O}_6$  (FW = 535.83), Yield: 63%, M.P. >300. Color: reddish brown, Molar conductance ( $\Lambda$ ) is  $9.2 \Omega^{-1}\text{cm}^2\text{mol}^{-1}$ . *Elemental Anal.* Calcd.% C, 51.60; H, 3.77; N, 15.70; Co, 11.05; Found % C, 52.39.; H, 3.79; N, 15.78; Co, 10.89; IR (KBr,  $\text{cm}^{-1}$ ): 3407 (br)  $\nu(\text{OH})$ , 3294, 3100  $\nu(\text{NH})$ , 1604  $\nu(\text{C}=\text{N})$ , 1250  $\nu(\text{C}-\text{O})_{\text{ph}}$ , 1009  $\nu(\text{N}-\text{N})$ , 578  $\nu(\text{M} \leftarrow \text{O})$ , 508  $\nu(\text{M} \leftarrow \text{N})$ , 1545, 1338 ( $\Delta = 207$ )  $\nu_{\text{sym}} \text{CH}_3\text{COO}$ ,  $\nu_{\text{asym}} \text{CH}_3\text{COO}$ .

**Manganese(II) complex (9)**,  $[\text{Mn}(\text{H}_2\text{L})_2]$ ,  $\text{C}_{42}\text{H}_{34}\text{MnN}_{12}\text{O}_8$  (FW = 889.75), Yield: 59%, M.P. >300. Color: dark yellow, Molar conductance ( $\Lambda$ ) is  $6.6 \Omega^{-1}\text{cm}^2\text{mol}^{-1}$ . *Elemental Anal.* Calcd.: C, 56.70; H, 3.85; N, 18.89; Mn, 6.17; Found: C, 56.52.; H, 3.56; N, 18.44; Mn, 5.89; IR spectra (KBr,  $\text{cm}^{-1}$ ): 3181, 3100  $\nu(\text{NH})$ , 1606  $\nu(\text{C}=\text{N})$ , 1514  $\nu(\text{N}=\text{C}-\text{O})$ , 1464  $\nu(\text{N}=\text{N})$ , 1242  $\nu(\text{C}-\text{O})_{\text{ph}}$ , 1006  $\nu(\text{N}-\text{N})$ , 576  $\nu(\text{M}-\text{O})$ , 490  $\nu(\text{M} \leftarrow \text{N})$ .

**Iron(III) complex (10)**,  $[\text{Fe}(\text{H}_2\text{L})_2\text{Cl}(\text{H}_2\text{O})]$ ,  $\text{C}_{42}\text{H}_{36}\text{FeClN}_{12}\text{O}_{10}$  (FW = 944.12), Yield: 65%, M.P. >300. Color: dark brown, Molar conductance ( $\Lambda$ ) is  $14.5 \Omega^{-1}\text{cm}^2\text{mol}^{-1}$ . *Elemental Anal.* Calcd.% C, 53.43; H, 3.84; N, 17.80; Fe, 5.92; Cl, 3.75; Found % C, 52.99.; H, 3.77; N, 17.51; Fe, 6.00 Cl, 3.25; IR (KBr,  $\text{cm}^{-1}$ ): 3432  $\nu(\text{H}_2\text{O})$ , 3360, 3259  $\nu(\text{NH})$ , 1694  $\nu(\text{C}=\text{O})$ , 1606  $\nu(\text{C}=\text{N})$ , 1485  $\nu(\text{N}=\text{N})$ , 1271  $\nu(\text{C}-\text{O})_{\text{ph}}$ , 969  $\nu(\text{N}-\text{N})$ , 563

$\nu(\text{M}\leftarrow\text{O})$ , 505  $\nu(\text{M}\leftarrow\text{N})$ .

**Ruthenium(III) complex (11)**,  $[\text{Ru}(\text{H}_2\text{L})_2\text{Cl}(\text{H}_2\text{O})]\text{C}_{42}\text{H}_{36}\text{RuClN}_{12}\text{O}_{10}$  (FW = 989.35), Yield: 61%, M.P. >300. Color: dark brown, Molar conductance ( $\Lambda$ ) is  $21.5 \Omega^{-1}\text{cm}^2\text{mol}^{-1}$ . *Elemental Anal.* Calcd.: C, 50.99; H, 3.58; N, 16.99; Ru, 10.22; Found % C, 50.56.; H, 3.26; N, 16.49; Ru, 10.25; IR spectra (KBr,  $\text{cm}^{-1}$ ): 3431  $\nu(\text{H}_2\text{O})$ , 3358, 3251  $\nu(\text{NH})$ , 1690  $\nu(\text{C}=\text{O})$ , 1583  $\nu(\text{C}=\text{N})$ , 1485  $\nu(\text{N}=\text{N})$ , 1280  $\nu(\text{C}-\text{O})_{\text{ph}}$ , 970  $\nu(\text{N}-\text{N})$ , 562  $\nu(\text{M}\leftarrow\text{O})$ , 513  $\nu(\text{M}\leftarrow\text{N})$ .

**Zinc(II) complex (12)**,  $[\text{Zn}(\text{H}_2\text{L})(\text{CH}_3\text{COO})]$ ,  $\text{C}_{23}\text{H}_{20}\text{ZnN}_6\text{O}_6$  (FW = 541.83), Yield: 58%, M.P. >300. Color: dark yellow, Molar conductance ( $\Lambda$ ) is  $7.54 \Omega^{-1}\text{cm}^2\text{mol}^{-1}$ . *Elemental Anal.* Calcd.% C, 50.99; H, 3.72; N, 15.51; Zn, 12.07; Found % C, 50.61.; H, 3.74; N, 15.11; Zn, 11.81; IR spectra (KBr,  $\text{cm}^{-1}$ ): 3432  $\nu(\text{OH})$ , 3287, 3102  $\nu(\text{NH})$ , 1614  $\nu(\text{C}=\text{N})$ , 1455  $\nu(\text{N}=\text{N})$ , 1253  $\nu(\text{C}-\text{O})_{\text{ph}}$ , 1013  $\nu(\text{N}-\text{N})$ , 582  $\nu(\text{M}\leftarrow\text{O})$ , 458  $\nu(\text{M}\leftarrow\text{N})$ , 1546, 1336 ( $\Delta = 200$ )  $\nu_{\text{sym}} \text{CH}_3\text{COO}$ ,  $\nu_{\text{asym}} \text{CH}_3\text{COO}$ .

**Uranium (VI) complex (13)**,  $[\text{UO}_2(\text{H}_2\text{L})_2]\text{C}_{42}\text{H}_{34}\text{UO}_2\text{N}_{12}\text{O}_8$  (FW = 1180.93), Yield: 59%, M.P. >300. Color: orange, Molar conductance ( $\Lambda$ ) is  $9.5 \Omega^{-1}\text{cm}^2\text{mol}^{-1}$ . *Elemental Anal.* Calcd.% C, 42.72; H, 3.93; N, 14.23; Found % C, 42.38.; H, 3.72; N, 13.97; IR spectra (KBr,  $\text{cm}^{-1}$ ): 3411  $\nu(\text{H}_2\text{O})$ , 3215, 3115  $\nu(\text{NH})$ , 1608  $\nu(\text{C}=\text{N})$ , 1518  $\nu(\text{N}=\text{C}-\text{O})$ , 1460,  $\nu(\text{N}=\text{N})$ , 1259  $\nu(\text{C}-\text{O})_{\text{ph}}$ , 1009  $\nu(\text{N}-\text{N})$ , 578  $\nu(\text{M}-\text{O})$ , 485  $\nu(\text{M}\leftarrow\text{N})$ .

#### *In-vitro antimicrobial activity*

The antimicrobial activities of the ligand and its metal complexes were carried out in the Botany Department Lab. of Microbiology, Faculty of Science, El-Menoufia University. They have been studied for their antimicrobial activities by Well Diffusion Method [22]. The antibacterial activities were done using *Escherichia coli* (*E. coli*) and *Bacillus subtilis* (*B. subtilis*) while the antifungal activity was done using Fungus (*Aspergillus niger*), at 250, 200 and 150  $\mu\text{g}/\text{mL}$  concentrations in solvent DMSO. Where DMSO poured disc was used as a negative control. The bacteria were subcultured in nutrient agar medium which, prepared using (g.L<sup>-1</sup> distilled water) NaCl (5 g), peptone (5 g), beef extract (3 g), agar (20 g). while the fungus was subcultured in Czapek Dox's medium which was prepared using (g.L<sup>-1</sup> distilled water) yeast extract (1g), sucrose (30 g), NaNO<sub>3</sub>, agar (20 g), KCl (0.5 g), KH<sub>2</sub>PO<sub>4</sub> (1 g), MgSO<sub>4</sub>·7H<sub>2</sub>O (0.5 g) and trace of FeCl<sub>3</sub>·6H<sub>2</sub>O. This medium was then

sterilized by autoclaving at 120 °C for 15 min. After cooling to 45 °C the medium was poured into 90 mm diameter Petri dishes and incubated at 28 °C. After solidifying, Petri dishes were stored at 4 °C for a few hours. Microorganisms were spread over each dish by using a sterile bent Loop rod. Disks were cut by the sterilized Cork borer and then taken by sterilized needle. The resulted pits are sites for the tested compounds of known concentration. Standard antibacterial drug (Tetracycline) antifungal drug (Nystatin) and solution of metal salts were also screened under similar conditions for comparison. Plates were allowed to stand in a refrigerator for two hours before incubation to allow the tested compounds to diffuse through the agar. The Petri dishes were incubated for 48 h at 28. The growth inhibition zones around the holes were observed, indicating that the examined compound inhibits the growth of microorganisms. The inhibition zone was measured in millimeters carefully. All determination was made in duplicate for each of the compounds. An average of the two independent readings for each compound was recorded.

#### **Results and Discussion**

The reaction of 2-(phenylamino) acetohydrazide with 2-hydroxy-4-((4-nitrophenyl) diazenyl) benzaldehyde in EtOH 1:1 mole ratio led to the formation of ligand H<sub>3</sub>L<sup>1</sup> (**1**), as shown in Figure 1. The reaction of the ligand (**1**) with metal salts using (1:1) mole ratios in the presence of triethylamine (2 mL) gives complexes; (**2**), (**6**), (**9-11**) and (**13**) however, (1:1) in the absence of triethylamine, it gives complexes; (**3-5**), (**7-8**) and (**12**) with different geometries. All the compounds are intensely colored, crystalline solids and stable at room temperature and don't decompose after prolonged storage. The complexes are insoluble in water, ethanol, methanol, benzene, toluene acetonitrile, and chloroform, but completely soluble in dimethylformamide (DMF) or dimethylsulfoxide (DMSO). Elemental analyses, spectroscopic techniques, and ESR spectra, which presented in the experimental part and tables 1&2 are compatible with the suggested structures as shown in Figures 2-6. The elemental analyses confirmed that the complexes (**2**), (**6**), (**9-11**) and (**13**) were composed in molar ratio 1L:1M, whereas the complexes (**3-5**), (**7-8**) and (**12**) were found to be formed in molar ratio 2L:1M.

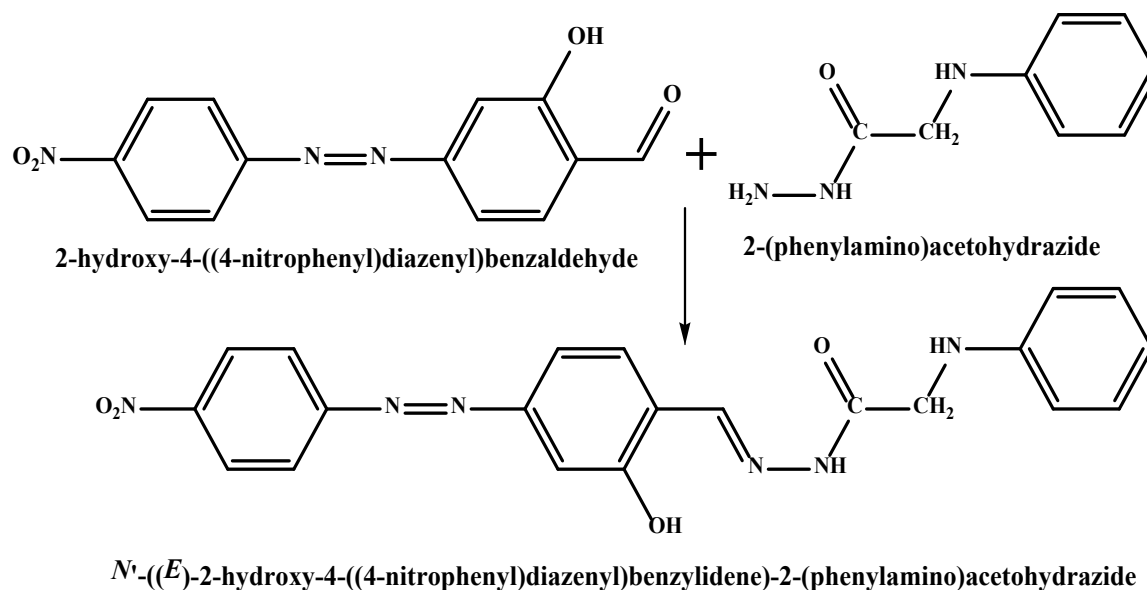
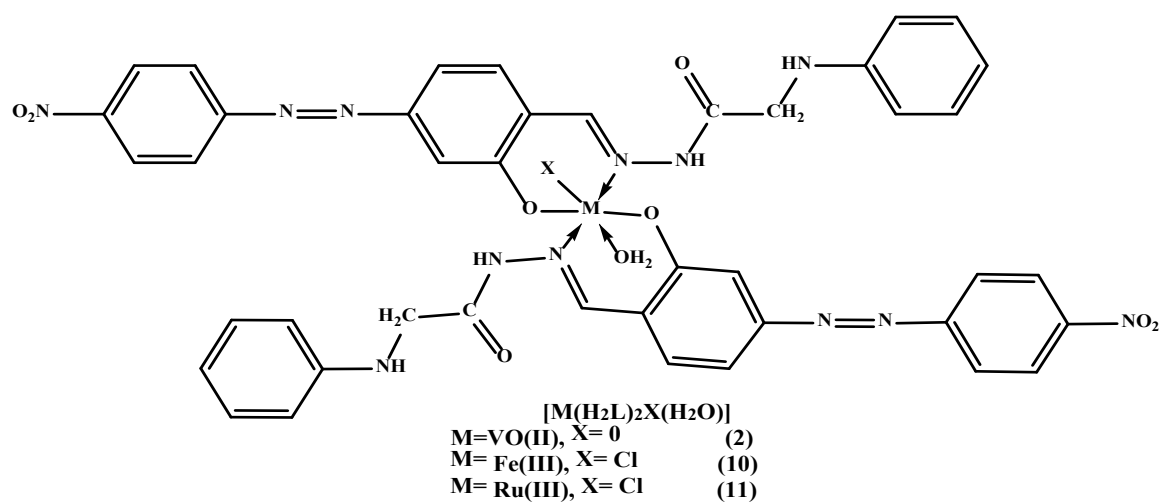
Fig.1. Scheme. The preparation of the ligand ( $H_3L$ , 1).

Fig. 2. Structural representation of VO(II), Fe(III) and Ru(III) complexes (2), (10) and (11).

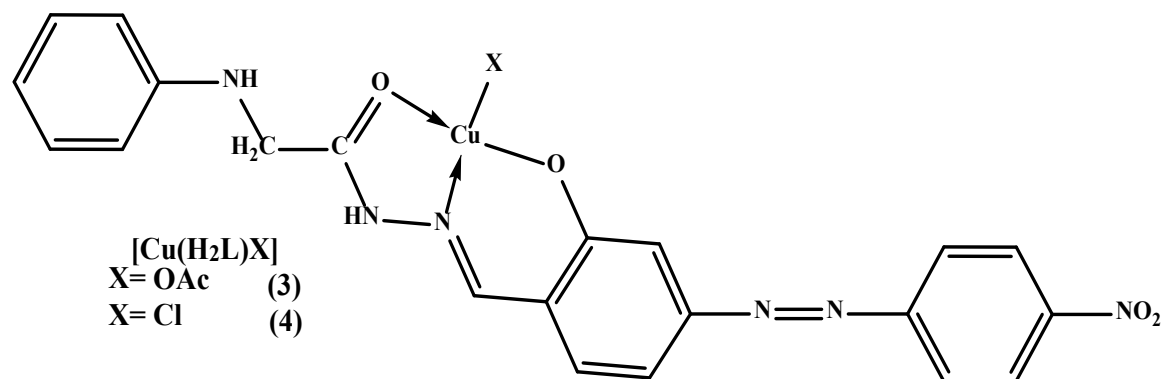


Fig.3. Structural representation of Cu(II) complexes (3) and (4).

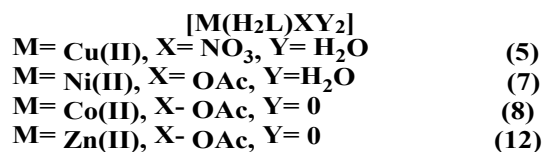
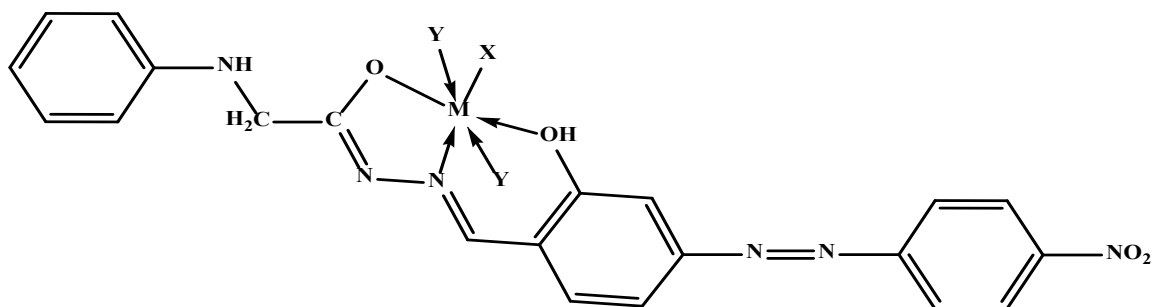


Fig. 4. Structural representation of Cu(II), Ni(II), Co(II) and Zn(II) complexes (5) (7-8) and (12).

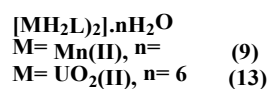
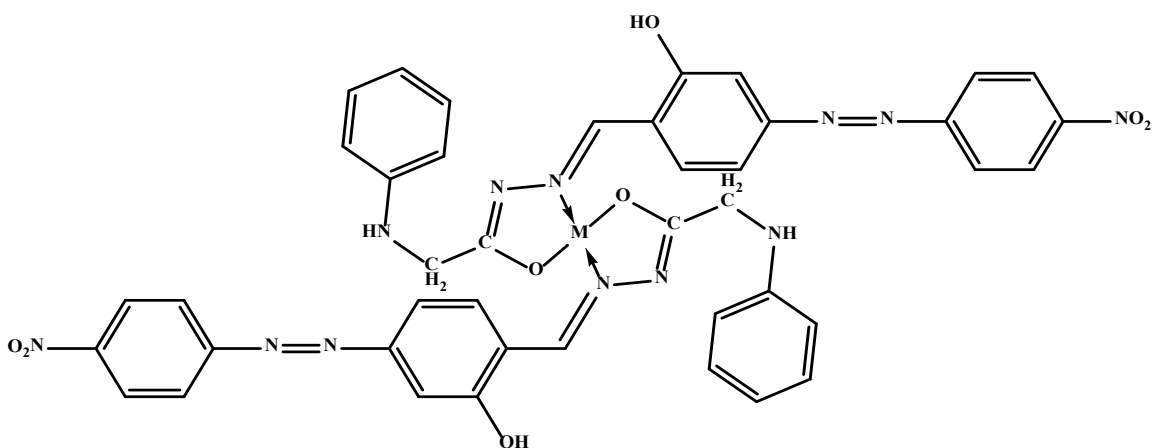


Fig.5. Structural representation of Mn(II) and UO<sub>2</sub>(II) complexes (9) and (13).

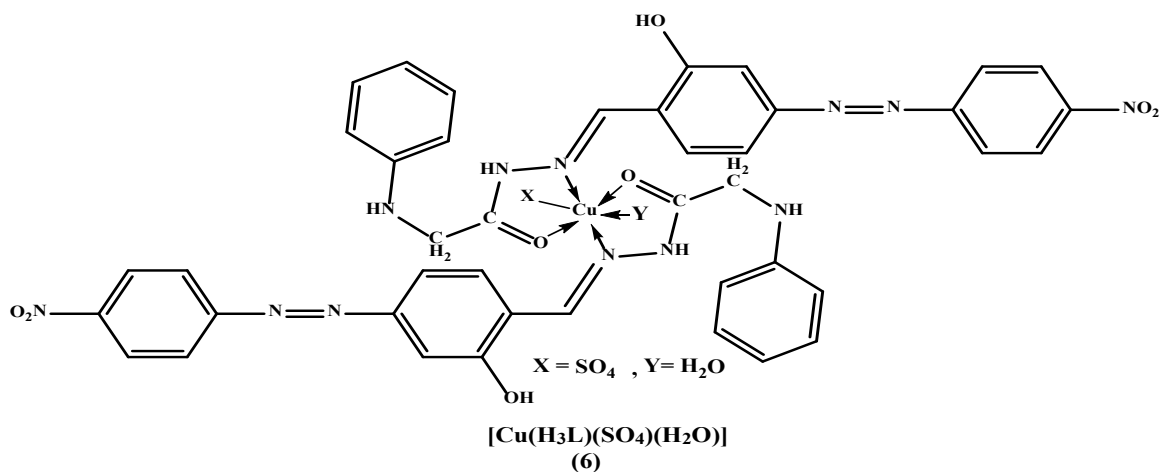


Fig.6. Structural representation of Cu(II) complex (6).

### <sup>1</sup>H- and <sup>13</sup>C-NMR spectra of ligand

The <sup>1</sup>H-NMR spectrum of the ligand in DM-SO-d<sub>6</sub> as a solvent showed signals, which are consistent with the proposed values. The spectrum of the ligand showed the absence of the signal of the amino group (-NH<sub>2</sub>) characteristic to the starting material (hydrazide). The spectrum showed three sets of peaks, the first one observed as a singlet at 5.2 (s, H) and 7.85 (s, 1H), 4.3(s, 1H) ppm, which may be assigned to the hydroxyl (OH), (-C=N-NH), and (ph-NH) protons respectively. [23,24] This assignment confirmed by the deuterated spectra in which the intensity of these bands is considerably decreased. The second set appeared as a singlet at 8.1 (s, 1H) ppm, which can be assigned to the azomethine proton (H-C=N) [24,25]. The third one appeared as multiples in the 6.43–8.19 (m, 12H) ppm range, which attributed to aromatic protons. It was clear from the <sup>1</sup>H-NMR spectrum of the ligand that it exhibits the keto form only and no evidence for the presence of the enol form. This result was confirmed from the appearance of the signal of the (NH) and phenolic (OH) only and the absence of the (OH) signal of the enolic form. The same conclusion was reported by many authors[24] The <sup>13</sup>C-NMR spectrum showed different peaks appearing at 173 and 161.3 ppm. These peaks can be attributed to C=O and -C-OH groups respectively[25,26]. The peaks at 150.6, 143.5 ppm assignable to CH=N- and C-NH group[22]. However, the peaks at 111. -139.1 ppm range assigned to the carbon of aromatic carbons[27].

### Conductivity Measurements

The molar conductivity of 1×10<sup>-3</sup>M solution of the metal complexes in DMSO at room temperature showed low conductivity (6.6–25.5 Ω<sup>-1</sup>cm<sup>2</sup>mol<sup>-1</sup> range (Table 1) indicating the non-electrolytic nature of these complexes. This confirmed that the anions of these complexes are coordinated to metal ion [28].

### IR Spectra

The bonding mode of the ligand in the metal complexes has been deduced from their IR spectra. Important spectral bands of the ligand and its metal complexes are presented in the experimental part. The spectrum of the ligand (H<sub>3</sub>L) showed a strong band at 3409 cm<sup>-1</sup> may be assigned to the ν(NH) group, whereas the strong band at 1694 cm<sup>-1</sup> due to the carbonyl group of the hydrazide moiety [22,23]. This observation indicates that the ligand is present in the ketonic form in the solid-state [29,30]. The spectrum showed a sharp band in the 3359 cm<sup>-1</sup>, which may be

assigned to the stretching vibration of the phenolic hydroxyl group [22]. The relatively strong and medium bands, which located at 3258, 3100, 1607, 1485 and 970 cm<sup>-1</sup> corresponded to the amine groups (N-NH), (CH<sub>2</sub>-NH), azomethine group[31], azo group[32], and ν(N-N)[22] respectively. The band, which appeared at 1257 cm<sup>-1</sup> is due to the ν(C-OH) of the phenolic moiety [30]. The mode of bonding of the ligand can be predicted by comparison the IR spectra of the complexes with that of the free ligand. The IR spectra data obtained for complexes showed that the ligand behaves as either of the following:

1) Neutral bidentate as in the case of complex **(6)** in which the ligand coordinated to metal ions via hydroxyl group and the azomethine nitrogen atom. The IR spectra of the sulfate complex **(6)** have new bands, which appeared at 1257, 1193, 1158, 869 cm<sup>-1</sup>. These bands indicate that the sulphate ion is coordinated to the copper<sup>(II)</sup> [33-36]. This mode of coordination was suggested by the following evidence: i) the band characteristic to ν(NH) and carbonyl group were still present and the band of the hydroxyl group is appeared as medium indicating that, in these complexes, the ligand coordinated to metal ion via hydroxyl group: ii) the band characteristic to azomethine group ν(C=N) appeared as weak band. At the same time, the band due to ν(N-N) was shifted to a higher frequency in the 980 cm<sup>-1</sup>. The increase in the frequency of this band ν(N-N) is a clear indication to the increase in the double bond character is off-setting the loss of electron density via electron donation to the metal ions and further confirmation of the coordination of the ligand via the azomethine group [31].

2) monobasic tridentate bonding through the enolic carbonyl oxygen (C-O), oxygen of hydroxyl group and azomethine nitrogen (C=N) atoms as in complexes **(5)** and **(7-9)**. This mode of bonding was suggested by the following evidence: i) The bands characteristic to the carbonyl ν(C=O), and ν(NH) groups disappeared indicating that the ligand bonded to the metal ions in its enolic form via enolic carbonyl oxygen atom, which is further supported by the appearance of new bands in the 1514–1523 and 1372–1380 cm<sup>-1</sup> ranges corresponding to the ν(N=C-O) and ν(C-O), respectively[33]. ii) The band characteristic to azomethine group ν(C=N) shifted or appeared as a weak band in the 1603-1607 cm<sup>-1</sup>. At the same time, the band due to ν(N-N) was shifted to a higher frequency and appearing in the 1009-1023 cm<sup>-1</sup> range. The increase in the frequency of this band ν(N-N) is a clear indication to the increase in the double bond character is off-setting the loss of electron density via electron

Table 1:- The analytical and some physical characteristics for the ligand H<sub>3</sub>L and its complexes.

No.	Ligand/complexes	Color	M.P. (°C)	M. Wt.	Calcd (Found) %			Cl/S	M	$\Lambda_M^a$	Yield (%)
					C	H	N				
1	C <sub>21</sub> H <sub>18</sub> N <sub>6</sub> O <sub>4</sub> (H <sub>3</sub> L)	D. Yellow	295	418.41	60.28 (59.79)	4.34 (4.18)	20.09(19.66)	--	--	--	85
2	[VO(H <sub>2</sub> L) <sub>2</sub> (H <sub>2</sub> O)]	L. Brown	>300	919.77	54.84 (53.99)	3.95 (3.89)	18.27(17.90)	--	5.54 (5.32)	25.5	55
3	[Cu(H <sub>2</sub> L)(CH <sub>3</sub> COO)]	Brown	>300	540.00	51.16 (50.69)	3.73 (3.45)	15.56 (15.25)	--	11.77(11.55)	13.3	67
4	[Cu(H <sub>2</sub> L)Cl]	Green	>300	516.40	48.84 (48.68)	3.32 (3.08)	16.27(15.99)	6.86(6.19)	12.31 (12.25)	15.4	62
5	[Cu(H <sub>2</sub> L)(NO <sub>3</sub> )(H <sub>2</sub> O) <sub>2</sub> ]	Olive	>300	578.99	43.56 (43.52)	3.66 (3.92)	16.93 (16.21)	--	10.98 (10.59)	12.1	55
6	[Cu(H <sub>3</sub> L) <sub>2</sub> (SO <sub>4</sub> )(H <sub>2</sub> O)]	Olive	>300	1014.44	49.73 (50.60)	3.78 (3.49)	16.57(16.25)	3.16(2.88)	6,26(5.89)	9.9	61
7	[Ni(HL)(H <sub>2</sub> O)].H <sub>2</sub> O	Brown	>300	571.17	48.37 (48.80)	4.24 (4.42)	14.71 (14.25)	--	10.28(10.21)	13.3	67
8	[Co(HL)(H <sub>2</sub> O)]	blue	>300	535.38	51.60 (52.39)	3.77 (3.79)	15.70 (15.78)	--	11.05 (10.89)	9.2	63
9	[Mn(H <sub>2</sub> L) <sub>2</sub> ]	D. yellow	>300	889.75	56.70(56.52)	3.85(3.56)	18.89 (18.44)	--	6.17 (5.89)	6.6	59
10	[Fe(H <sub>2</sub> L) <sub>2</sub> Cl(H <sub>2</sub> O)]	D. Brown	>300	944.12	53.43 (52.99)	3.84 (3.77)	17.80(17.51)	3.75(3.25)	5.92(6.00)	14.5	65
11	[Ru(H <sub>2</sub> L) <sub>2</sub> Cl(H <sub>2</sub> O)]	D. Brown	>300	989.35	50.99 (50.56)	3.58 (3.26)	16.99(16.49)	3.58(3.28)	10.22(10.25)	21.5	61
12	[Zn(H <sub>2</sub> L)(CH <sub>3</sub> COO)]	D. Yellow	>300	541.83	50.99 (50.61)	3.72 (3.74)	15.51 (15.11)	--	12.07 (11.812)	7.5	58
13	[(UO <sub>2</sub> )(H <sub>2</sub> L) <sub>2</sub> ].6H <sub>2</sub> O	Orange	>300	1180.93	42.72 (42.38)	3.93 (3.72)	14.23(13.97)	--	20.16 (19.34)	9.5	59

<sup>a</sup> Molar conductivity as 10<sup>-3</sup> M solutions (ohm<sup>-1</sup> cm<sup>2</sup> mol<sup>-1</sup>), D.= dark, R. = Reddish

donation to the metal ions and further confirmation of the coordination of the ligand via the azomethine group [31]. iii) The appearance of new bands in the 561–620 and 458–513  $\text{cm}^{-1}$  ranges for all complexes may be assigned to the  $\nu(\text{M}-\text{O})$ ,  $\nu(\text{M}=\text{O})$  and  $\nu(\text{M}=\text{N})$  respectively [34]. The appearance of these bands was taken as confirmation of the bonding of the ligand with the metal ions that occurred via the carbonyl oxygen atom in enolic or ketonic form, azomethine nitrogen atom and/or deprotonated phenolic hydroxyl oxygen atom. Complexes **(3)**, **(7-8)** and **(12)** have shown that the acetate ion may be bonding to the metal ion in unidentate. The  $\nu_{\text{as}}(\text{CO}_2)$  and  $\nu_{\text{s}}(\text{CO}_2)$  of the free acetate ion are ca. 1560 and 1416  $\text{cm}^{-1}$  respectively. In unidentate acetate complexes  $\nu(\text{C}=\text{O})$  is the same as  $\nu_{\text{s}}(\text{CO}_2)$  in free acetate ion but  $\nu(\text{C}-\text{O})$  show 1338, 1336  $\text{cm}^{-1}$ . As a result, the separation between the free  $\nu(\text{CO})$  and  $\nu_{\text{as}}(\text{CO}_2^-)$  indicate that the acetate ion is bonding with metal ion as  $(\text{CH}_3\text{COO})$ .

#### Magnetic Moment

The magnetic moments of the complexes **(2)-(11)** at room temperature showed that all these complexes are paramagnetic. vanadyl<sup>(IV)</sup> complex **(2)** shows a magnetic value equal to 1.70 BM, which is corresponding to one unpaired electron [33,36]. The copper<sup>(II)</sup> complexes **(3)-(6)** show values in the 1.75–1.85 BM range, which are consistent with one unpaired electron system in octahedral environment [23]. Nickel(II) complex **(7)** shows the value of 2.95 BM, which is consistent with two unpaired electrons system of the octahedral nickel<sup>(II)</sup> complex [32]. Cobalt<sup>(II)</sup> complex **(8)** shows value 3.8 indicating a high spin cobalt<sup>(II)</sup> complex [37]. The magnetic moment values of manganese<sup>(II)</sup> and iron<sup>(III)</sup> complexes **(9)** and **(10)** are 1.92 and 5.90 BM, respectively suggesting square planar geometry around the manganese(II) and octahedral iron<sup>(III)</sup> complexes. The magnetic moment value of the ruthenium<sup>(III)</sup> complex **(11)** is 1.95 BM, which is characteristic of  $d^5$  low spin ruthenium<sup>(III)</sup> complex [37].

#### Electronic Spectra

The electronic spectral data of the ligand and its metal complexes in DMF solutions are summarized in Table 3. The ligand showed that the two lone pairs of electrons of the azo group are not the only interacting non-bonding electrons. Since the ligand is hydrazone, part of it contains nitrogen and oxygen atoms, which also may be extra sources of lone pair of electrons. Thus, this type of transition,  $n \rightarrow \pi^*$  is expected to take place from these non-bonding orbitals to

different molecular orbitals extending over such large molecules [38]. The data reveals that; the ligand comprises three sets of bands in the UV and visible regions. The first set of the shortest wavelength appeared at 220 and 250 nm may be assigned to the  $\pi \rightarrow \pi^*$  transition in the benzenoid and Intra ligand  $\pi \rightarrow \pi^*$  transition [26,37]. The second set appeared at 325 and 3350 nm may be assigned to  $n \rightarrow \pi^*$  transition of the azomethine and carbonyl group [26,37]. The third set located at 375 nm may be ascribed to  $\pi \rightarrow \pi^*$  transition involving the  $\pi$  electron of the azo group [38,39]. The band located in the visible region at 410 nm can be assigned to  $\pi \rightarrow \pi^*$  transition involving the whole electronic system of the compounds with a considerable charge transfer character arising mainly from the phenolic moiety [38,39]. The spectrum of vanadyl(II) complex **(2)** showed that, there are three bands at 510, 565, 690 nm assigned to  ${}^2\text{B}_2(d_{xy}) \rightarrow {}^2\text{A}_1(dz^2)$ ,  ${}^2\text{B}_2(d_{xy}) \rightarrow {}^2\text{B}_1(d_{x^2-y^2})$  and  ${}^2\text{B}_2(d_{xy}) \rightarrow \text{E}(d_{xz}, d_{yz})$  transitions, which confirmed that, the vanadyl(II) complex has a distorted octahedral structure [40-43]. The spectrum of copper complexes **(3,4)** displayed a broadband around 500 nm, which may be assigned to  ${}^2\text{B}_{1g} \rightarrow {}^2\text{A}_{1g}$  transition and suggested to square planar geometry around the copper(II) ion [40,41], whereas the electronic spectrum of copper(II) complexes **(5,6)** in DMF solution showed a broad band centered at 590–550 nm corresponding to  ${}^2\text{E}_g \rightarrow {}^2\text{T}_{2g}$  transition, which confirmed distorted octahedral geometry [40,42]. Nickel(II) complex **(7)** exhibits three bands located at 510, 570, 710 nm, which may be assigned to  ${}^3\text{A}_{2g}(\text{F}) \rightarrow {}^3\text{T}_{1g}(\text{P})(v_3)$ ,  ${}^3\text{A}_{2g}(\text{F}) \rightarrow {}^3\text{T}_{1g}(\text{F})(v_2)$  and  ${}^3\text{A}_{2g}(\text{F}) \rightarrow {}^3\text{T}_{2g}(\text{F})(v_1)$ , which are characteristic to nickel(II) ion in an octahedral structure [40,43,44]. The  $v_2/v_1$  ratio for the complex is 1.36, which is less than the usual range of 1.5-1.75, indicating a distorted octahedral nickel(II) complex [44]. The cobalt(II) complex **(8)** showed a weaker broad absorption band at 590 nm assigned to  ${}^4\text{T}_{1g}(\text{F}) \rightarrow {}^4\text{T}_{1g}(\text{P})$  transition of octahedral geometry [40,42]. The manganese(II) complex **(9)** displays two weak absorption bands at 390 and 490 nm assigned to  ${}^6\text{A}_{1g} \rightarrow {}^4\text{A}_{1g}$  and  ${}^6\text{A}_{1g} \rightarrow {}^4\text{T}_{2g}$  respectively, suggesting tetrahedral geometry of manganese(II) [45,46]. The iron(III) complex **(10)** gave four bands at 530, 480, 410 and 390 nm which due to  ${}^6\text{A}_{1g} \rightarrow {}^4\text{T}_{2g}$ ,  ${}^6\text{A}_{1g} \rightarrow {}^4\text{T}_1(\text{G})$ ,  ${}^6\text{A}_{1g} \rightarrow {}^4\text{Eg}(\text{G})$  and  ${}^6\text{A}_{1g} \rightarrow {}^4\text{A}_{1g}(\text{G})$ , transitions. These bands are characteristic of the octahedral iron(III) complex [40-44]. However the electronic absorption spectrum of ruthenium(III) complex **(11)** displayed two bands at 520 and 650 nm. The first band is due to LMCT transition and

Table 2. The IR spectral ( $\text{cm}^{-1}$ ) assignment for the ligand  $\text{H}_2\text{L}$  and its metal complexes.

No.	Ligand/complexes	$\nu(\text{OH}/\text{H}_2\text{O})$	$\nu(\text{NH})$	$\nu(\text{C}=\text{O})$	$\nu(\text{C}=\text{N})$	$\nu(\text{N}=\text{C}-\text{O})$	$\nu(\text{C}-\text{O})_{\text{as}}$	$\nu(\text{NO}_2)$	$\nu(\text{N}-\text{N})$	$\nu(\text{M}-\text{O})$	$\nu(\text{M}-\text{N})$
1	$\text{C}_{21}\text{H}_{18}\text{N}_6\text{O}_4$ ( $\text{H}_3\text{L}$ )	3409(w)	3359, 3258, 3100	1694	1607	--	1257	--	970	--	--
2	$[\text{VO}(\text{H}_2\text{L})_2(\text{H}_2\text{O})]$	3423(br)	3360, 3259, 3100	1694	1609	--	1270	--	970	561	505
3	$[\text{Cu}(\text{H}_2\text{L})(\text{CH}_3\text{COO})]$	3433(br)	3363, 3261, 3090	1987	1605	--	1285	1522, 1338(184)	978	590	505
4	$[\text{Cu}(\text{H}_2\text{L})\text{Cl}]$	3434(br)	3360, 3259, 3100	1693	1605	--	1277	--	965	620	499
5	$[\text{Cu}(\text{H}_2\text{L})(\text{NO}_3)(\text{H}_2\text{O})_2]$	3434(br)	3343, 3110	--	1605	1523	1257	1466, 1373(93)	1023	590	478
6	$[\text{Cu}(\text{H}_2\text{L})_2(\text{SO}_4)(\text{H}_2\text{O})]$	3433	3356, 3259, 3106	1694	1605	--	1288	1193, 1023, 896	980	590	467
7	$[\text{Ni}(\text{HL})(\text{CH}_3\text{COO})(\text{H}_2\text{O})_2]$	3421	3272, 3101	--	1604	1518	1257	1540, 1336(204)	1018	566	489
8	$[\text{Co}(\text{HL})(\text{CH}_3\text{OO})]$	3407	3294, 3100	--	1604	1519	1250	1545, 1338(207)	1009	578	508
9	$[\text{Mn}(\text{H}_2\text{L})_2]$	3420	3181, 3100	--	1606	1514	1242	--	1006	576	490
10	$[\text{Fe}(\text{H}_2\text{L})_2\text{Cl}(\text{H}_2\text{O})]$	3432	3360, 3259	1694	1606	--	1271	--	969	563	505
11	$[\text{Ru}(\text{H}_2\text{L})_2\text{Cl}(\text{H}_2\text{O})]$	3431	3358, 3251	1690	1583	--	1280	--	970	562	513
12	$[\text{Zn}(\text{H}_2\text{L})(\text{CH}_3\text{COO})]$	3432	3287, 3102	--	1614	1517	1253	1546, 1336(200)	1013	582	458
13	$[(\text{UO}_2)(\text{H}_2\text{L})_2] \cdot 6\text{H}_2\text{O}$	3411	3215, 3115	--	1608	1518	1259	1547, 1339(198)	1009	578	485

Ph. = phenolic, a. =Amide

### Electronic Spectra

The electronic spectral data of the ligand and its metal complexes in DMF solutions are summarized in Table 3. The ligand showed that the two lone pairs of electrons of the azo group are not the only interacting non-bonding electrons. Since the ligand is hydrazone, part of it contains nitrogen and oxygen atoms, which also may be extra sources of lone pair of electrons. Thus, this type of transition,  $n \rightarrow \pi^*$  is expected to take place from these non-bonding orbitals to different molecular orbitals extending over such large molecules [38]. The data reveals that; the ligand comprises three sets of bands in the UV and visible regions. The first set of the shortest wavelength appeared at 220 and 250 nm may be assigned to the  $\pi \rightarrow \pi^*$  transition in the benzenoid and Intra ligand  $\pi \rightarrow \pi^*$  transition [26,37]. The second set appeared at 325 and 3350 nm may be assigned to  $n \rightarrow \pi^*$  transition of the azomethine and carbonyl group [26,37]. The third set located at 375 nm may be ascribed to  $\pi \rightarrow \pi^*$  transition involving the  $\pi$  electron of the azo group [38,39]. The band located in the visible region at 410 nm can be assigned to  $\pi \rightarrow \pi^*$  transition involving the whole electronic system of the compounds with a considerable charge transfer character arising mainly from the phenolic moiety [38,39]. The spectrum of vanadyl(II) complex(2) showed that, there are three bands at 510, 565, 690 nm assigned to  ${}^2B_2(d_{xy}) \rightarrow {}^2A_1(dz^2)$ ,  ${}^2B_2(d_{xy}) \rightarrow {}^2B_1(d_{x^2-y^2})$  and  ${}^2B_2(d_{xy}) \rightarrow E(d_{xz}, d_{yz})$  transitions, which confirmed that, the vanadyl(II) complex has a distorted octahedral structure [40-43]. The spectrum of copper complexes (3,4) displayed a broadband around 500 nm, which may be assigned to  ${}^2B_{1g} \rightarrow {}^2A_{1g}$  transition and suggested to square planar geometry around the copper(II) ion [40,41], whereas the electronic spectrum of copper(II) complexes (5,6) in DMF solution showed a broad band centered at 590–550 nm corresponding to  ${}^2E_g \rightarrow {}^2T_{2g}$  transition, which confirmed distorted octahedral geometry [40,42]. Nickel(II) complex (7) exhibits three bands located at 510, 570, 710 nm, which may be assigned to  ${}^3A_{2g}(F) \rightarrow {}^3T_{1g}(P)$  ( $\nu_3$ ),  ${}^3A_{2g}(F) \rightarrow {}^3T_{1g}(F)$  ( $\nu_2$ ) and  ${}^3A_{2g}(F) \rightarrow {}^3T_{2g}(F)$  ( $\nu_1$ ), which are characteristic to nickel(II) ion in an octahedral structure [40,43,44]. The  $\nu_2 / \nu_1$  ratio for the complex is 1.36, which is less than the usual range of 1.5-1.75, indicating a distorted octahedral nickel(II) complex [44]. The cobalt(II) complex (8) showed a weaker broad absorption band at 590 nm assigned to  ${}^4T_{1g}(F) \rightarrow {}^4T_{1g}(P)$  transition of octahedral geometry [40,42]. The

manganese(II) complex (9) displays two weak absorption bands at 390 and 490 nm assigned to  ${}^6A_{1g} \rightarrow {}^4A_{1g}$  and  ${}^6A_{1g} \rightarrow {}^4T_{2g}$ , respectively, suggesting tetrahedral geometry of manganese(II) [45,46]. The iron(III) complex (10) gave four bands at 530, 480, 410 and 390 nm which due to  ${}^6A_{1g} \rightarrow {}^4T_{2g}$ ,  ${}^6A_{1g} \rightarrow {}^4T_1(G)$ ,  ${}^6A_{1g} \rightarrow {}^4E_g(G)$  and  ${}^6A_{1g} \rightarrow {}^4A_{1g}(G)$ , transitions. These bands are characteristic of the octahedral iron(III) complex [40-44]. However the electronic absorption spectrum of ruthenium(III) complex (11) displayed two bands at 520 and 650 nm. The first band is due to LMCT transition and the second is assigned to  ${}^2T_{2g} \rightarrow {}^2A_{2g}$  transition. The band positions are similar to those observed for other octahedral ruthenium(III) complexes [40,41]. The diamagnetic complexes zinc(II) (12) and uranyl (II) (13) do not show d-d transitions. The bands observed are due to intraligand transitions.

### ESR spectra (solid state):

The ESR spectra of copper complexes (2-6) and (8) are recorded at room temperature. The ESR spectra of the complexes showed lines in the low field region with axial symmetry type with two g-values indicating a  $d_{x^2-y^2}$  ground state which is the most common feature for copper(II) complexes [45,46]. These data show  $g_{\parallel} > g_{\perp} > 2.0023$  characteristics of a compound having an octahedral geometry around the copper(II) ion [47]. These lines were corresponding to the interaction of the unpaired each line for the others. The experimental ESR parameters of copper(II) complexes are presented in Table 4. The parameter G is calculated according to the equation  $G = (g_{\parallel} - 2.0023) / (g_{\perp} - 2.0023)$  and shows values  $> 4$ , indicating that there is no direct copper-copper interaction in the solid-state. The  $g_{\parallel} / A_{\parallel}$  is taken as an indication for the stereochemistry of the copper(II) complexes. Addison has suggested that this ratio may be an empirical indication of the tetrahedral distortion of the square planar geometry [48]. The values of  $g_{\parallel} / A_{\parallel}$  quotient in the range (105–135  $\text{cm}^{-1}$ ) are expected for copper complexes within perfectly square-based geometry and those higher than 150  $\text{cm}^{-1}$  for tetrahedrally distorted complexes. The values for the complexes under investigation, Table 4, indicate tetragonally distorted complexes [49,50]. In this work, the copper (II) complexes show  $\beta_1^2$  values in the range 0.76-0.88 indicating the covalent character of the in-plane n-bonding. Also, the complexes show  $\beta^2 > 1$  indicating the ionic character of the out-of-plane  $\pi$ -bonding [51].

TABLE 3. UV-Vis. spectra of the ligand (H<sub>2</sub>L) and its metal complexes.

No	Bands in DMF	Electronic transition	$\mu_{\text{eff}}$ (BM)	Geometry
1	220, 250, 325, 350, 375, 410	2B <sub>2</sub> (dxy)→2A <sub>1</sub> (dz <sup>2</sup> )		
2	245, 280, 310, 348, 375, 510, 565,590	2B <sub>2</sub> (dxy)→2B <sub>1</sub> (dx <sup>2</sup> -y <sup>2</sup> ) 2B <sub>2</sub> (dxy)→E(dxz,dyz)	1.70	octahedral
3	250, 330, 360, 390, 500	<sup>2</sup> B <sub>1g</sub> → <sup>2</sup> A <sub>1g</sub>	1.80	Square planar
4	250, 330, 360, 390, 500	<sup>2</sup> B <sub>1g</sub> → <sup>2</sup> A <sub>1g</sub>	1.78	Square planar
5	230, 250, 285, 330, 390, 620	<sup>2</sup> B <sub>1g</sub> → <sup>2</sup> A <sub>1g</sub>	1.75	distorted
6	233, 270, 335, 360, 394, 620	<sup>2</sup> B <sub>1g</sub> → <sup>2</sup> B <sub>2g</sub>	1.85	octahedral
7	,570 ,510 ,395 ,372 ,340 ,270 ,240 710	<sup>3</sup> A <sub>2g</sub> (F)→ <sup>3</sup> T <sub>1g</sub> (P)(v <sub>3</sub> ), <sup>3</sup> A <sub>2g</sub> (F)→ <sup>3</sup> T <sub>1g</sub> (F)(v <sub>2</sub> ) <sup>3</sup> A <sub>2g</sub> (F)→ <sup>3</sup> T <sub>2g</sub> (F)(v <sub>1</sub> )	2.95	octahedral
8	220, 240, 300, 350, 590	<sup>4</sup> T <sub>1g</sub> (F)→ <sup>4</sup> T <sub>1g</sub> (P)	3.8	octahedral
9	225, 240, 300,390 ,490	<sup>6</sup> A <sub>1g</sub> → <sup>4</sup> A <sub>1g</sub> <sup>6</sup> A <sub>1g</sub> → <sup>4</sup> T <sub>2g</sub>	5.90	tetrahedral
10	250, 320, 350, 380,410, 480,530	6A <sub>1g</sub> →4T <sub>2g</sub> 6A <sub>1g</sub> →4T <sub>1</sub> (G) 6A <sub>1g</sub> →4 E <sub>g</sub> (G) 6A <sub>1g</sub> →4A <sub>1g</sub> (G),	5.90	octahedral
11	250, 310, 370, 510, 565	LMCT 2T <sub>2g</sub> →2A <sub>2g</sub>	1.95	octahedral
12	220, 270, 305, 330, 347, 390		Dia.	
13	230, 275, 305, 400		Dia.	Octahedral

*Antibacterial and Antifungal Screening*

The ligand and its metal complexes have been screened for their antibacterial and antifungal activities at different concentrations using well diffusion method against *E. Coli* and *Aspergillus Niger* and the results obtained are presented in Table 5. It is observed that the activities of the compounds increase with increasing the concentration of the solutions as well as the metal complexes are more potent than the parent ligand. This enhancement in the activity can be explained based on the chelation theory [52,53]. Chelation reduces the polarity of the metal ion considerably, mainly because of the partial sharing of its positive charge with donor groups and possible  $\pi$ -electron delocalization on the whole chelate ring. The lipid and polysaccharides are some important constituents of cell walls and membranes, which are preferred for metal ion interaction. In addition to this, the cell wall also contains many amino phosphates, carbonyl, and cysteinyl ligands, which maintain the integrity of the membrane by acting as a diffusion barrier and provides suitable sites for binding. Chelation can reduce not only the polarity of the metal ion but also increases

the lipophilic character of the chelate and the interaction between metal ions and the lipid is favored. This may lead to the breakdown of the permeability barrier of the cell resulting in interference with the normal cell processes. If the geometry and charge distribution around the molecule are incompatible with geometry and charge distribution around the pores of the bacterial cell wall, penetration through the wall by the toxic agent cannot take place and this will prevent the toxic reaction within the pores. Chelation is not the only criterion for antibacterial activity. Some important factors such as the nature of the metal ion, nature of the ligand, coordinating sites, and geometry of the complex, concentration, hydrophobicity, lipophilicity and presence of co-ligands have considerable influence on antibacterial activity. Certainly, steric and pharmacokinetic factors also play a decisive role in deciding the potency of an antimicrobial agent. The results show that complex (10) exhibits higher antifungal activity, complex (7) exhibits higher antibacterial *E. Coli* than the other complexes and complex (10) show higher agent antibacterial *B.subtilis* than the other complexes.

TABLE 4. ESR parameters of vanadyl(II), copper(II) and manganese complexes.

No.	$g_{\parallel}$	$g_{\perp}$	$g_{iso}$	$A_{\parallel}(cm^{-1})$	$A_{\perp}(cm^{-1})$	$A_{iso}(cm^{-1})$	$g_{\parallel}/A_{\parallel}(cm^{-1})$	G
2			2.025					
3	---	---	2.061	---	---	---	---	---
4	---	---	2.112	---	---	---	---	---
5	---	---	2.106	---	---	---	---	---
6	2.22	2.042	2.10	$186 \times 10^{-4}$	$57 \times 10^{-4}$	$98 \times 10^{-4}$	119	5.03
8	---	---	2.120	---	---	---	---	---

**TABLE 5. Biological activities of the ligand and its metal complexes against bacteria and fungus.**

No.	Inhibition zone in mm		
	<i>A. niger</i>	<i>E. coli</i>	<i>B. subtilis</i>
DMSO	0	0	0
Nystatin	32	--	--
Tetracycline	--	35	38
1	9	8	6
2	11	9	15
3	0	0	0
4	0	9	13
5	12	15	15
6	11	14	18
7	12	23	14
8	0	0	8
9	12	15	17
10	15	18	20
11	12	10	15
12	13	17	18

**References**

- Amer J. J. and Saniab S. K. Synthesis, Spectral of Azo Dyes Complexes with Ni (II) and Cu (II) and Their Industrial and Bacteriological Application. *Inter. J. of Sci. and Res.*, **7**, 1291- 1297(2017)
- Xu G. C., Zhang L., Liu L., Liu G. F. and Jia D. Z. Syntheses, characterization and crystal structures of mixed-ligand Cu(II), Ni(II) and Mn(II) complexes of N-(1-phenyl-3-methyl-4-propenylidene-5-pyrazolone)-salicylidene hydrazide containing ethanol or pyridine as a coligand. *Polyhedron*, **27**, 12-24 (2008).
- Bhosale J. D., Shirolkar A. R., Pete U. D., Zade C. M., Mahajan D. P., Hadole C. D., Pawar S. D., Patil U. D., Dabur R. and Bendre R.S. Synthesis, characterization and biological activities of novel substituted formazans of 3,4-dimethyl-1Hpyrrole-2-carbohydrazide derivatives. *J. Pharm., Res.*, **7**, 582-587 (2013).
- Çay S., Köse M., Tümer F., Gölcü A. and Tümer M. SOD activity and DNA binding properties of a new symmetric porphyrin Schiff base ligand and its metal complexes. *Spectrochim., Acta Part A Mol., Biom., Spectro.*, **151**, 821-838 (2015).
- El-Tabl A.S., Shakdofa M. M. E. and Shakdofa A. M. E. Metal complexes of N'-[2-hydroxy-5-(phenyldiazenyl)-benzylidene]isonicotinohydrazide. Synthesis, spectroscopic characterization and antimicrobial activity. *J., Serb., Chem., Soc.*, **78**, 39-55(2013).
- Hayam A., Abd El Salam , Ehab M., Zayed M. A. and Zayed M. N. Synthesis, Structural Characterization, Thermal Behaviour and Antimicrobial Activity of Copper, Cadmium and Zinc Chelates of Traizole-thiole Ligand in Comparison with Theoretical Molecular Orbital Calculations. *Egypt., J., Chem.*, Vol. **62** Special Issue (Part 1) pp. 145 - 163 (2019)
- Netalkar P. P., Netalkar S. P., Budagumpi S. and Revankar V.K. Synthesis, crystal structures and characterization of late first row transition metal complexes derived from benzothiazole core: Anti-tuberculosis activity and special emphasis on DNA binding and cleavage property. *Eur., J., Med., Chem.*, **79**, 47-56.( 2014).
- Neelima P. K., Siddiqui S., Arshad M., and Kumar D. In vitro anticancer activities of Schiff base and its lanthanum complex. *Spectrochim. Acta Part A Mol., Biomol., Spectr.*, **155**, 146-154 (2016).
- Correia I., Adão P., Roy S., Wahba M., Matos C., Maurya M. R., Marques F., Pavan F.R., Leite, C. Q., and Avecilla F. Hydroxyquinoline derived vanadium(IV and V) and copper(II) complexes as potential anti-tuberculosis and anti-tumor agents. *J., Inorg., Biochem.*, **41**, 83-93 (2014).
- Badiger R. S., Hunoor B. R., Patil R. S., Vadavi V. M., Chandrashekar I. S., Muchchandi Y. P., Patil M., Nethaji K. B., Gudasi. Synthesis, spectroscopic properties and biological evaluation of transition metal complexes of salicylhydrazone of anthranilhydrazide: X-ray crystal structure of copper complex. *D. S. Inorg., Chim., Acta.* **384**, 197-203 (2012).
- Netalkar P. P., Netalkar S. P., Budagumpi S., Revankar V. K. Synthesis, crystal structures and characterization of late first row transition metal complexes derived from benzothiazole core: anti-tuberculosis activity and special emphasis on DNA binding and cleavage property. *Eur., J., Med., Chem.*, **22**, 47-56 (2014).

12. Patil B. R., Machakanur S. S., Rekha S. Hunoor D., Badiger S., Gudasi K. B., Annie Bligh S. W. Synthesis and anti-cancer evaluation of cyclotriphosphazene hydrazone derivatives, *Der., Pharma., Chemica.*, **3**, 377-388 (2011).
13. Aljamali N. M. Review in Azo Compounds and its Biological Activity. *Biochem., Anal., Biochem.*, **4(2)**:1-4 (2015).
14. Gaber M., Ayad M. M., El-Sayed Y. S. Synthesis, spectral and thermal studies of Co(II), Ni(II) and Cu(II) complexes containing azo-pyrimidine moiety. *Spectrochim., Acta A* **62**, 694-702 (2005).
15. Sharad D., Dakore V., Kamble and Parshuram P. Synthesis and characterization of biologically active N<sub>2</sub>O<sub>2</sub> type of Novel Schiff base metal complexes derived from 4-amino antipyrine using TEA. *Inter., J., of Chem., Stud.*, **5(1)**: 110-113 (2017)
16. Liu J. N., Wu B.W., Zhang B., Liu Y. Synthesis and characterization of metal complexes of Cu(II), Ni(II), Zn(II), Co(II), Mn(II) and Cd(II) with tetradentate schiff bases. *Turk., J., Chem.*, **30**, 41-48 (2006).
17. Al-Hakimi A. N., El-Tabl A. S. and Shakdofa M. M. E., Coordination and Biological Behavior of 2-(p-toluidino)-N'-(3-oxo-1,3-diphenylpropylidene) acetohydrazide and its Metal Complexes. *J., of Chem., Res.*, December 770-774 (2009).
18. Emam S. M., AbouEl-Enein S. A., El-Saied F.A., Alshater S.Y. Synthesis and characterization of some bi, tri and tetravalent transition metal complexes of N'-(furan-2-ylmethylene)-2-(p-tolylamino) acetohydrazide HL 1 and N'-(thiophen-2-yl-methylene)-2-(ptolylamino) acetohydrazide HL<sub>2</sub>. *Spectrochim., Acta Part A* **92**, 96 (2012).
19. Svehla G. Vogel's Textbook of macro and semimicro qualitative inorganic analysis, Longman London pp 241-268 (1979)
20. Welcher F. J. analytical uses of ethylenediaminetetraacetic acid. Van Nostrand. p 213-220 (1965).
21. Vogel A. A Text Book of Quantitative Inorganic Analysis, ELBS. Longman London, p 125-130 (1978).
22. Collee J. G., Mackie T. J., McCartney J. E. Practical Medical Microbiology. 14th ed., Churchill Livingstone: New York. p 978 (1996).
23. Collee G., Duguid J. P., Farser A.G., Marmion B.D. (Eds), Practical Medical Microbiology, Churchill Livingstone, New York. p89-96 (1989).
24. Gup R. and Kirkan B. Synthesis and spectroscopic studies of copper(II) and nickel(II) complexes containing hydrazone ligands and heterocyclic coligand. *Spectrochim., Acta Part A Mol. Biomol., Spectrosc.*, **62**, 1188-1195 (2005).
25. Maurya M. R., Khurana S., Schulzke C., Rehder D. Dioxo- and oxovanadium(V) complexes of biomimetic hydrazone ONO donor ligands: Synthesis, characterisation, and reactivity. *Eur., J., Inorg., Chem.*, **3**, 779-788 (2001).
26. Bessy R., Prathapachandra B. N., Kurup M. R., Suresh E. Synthesis, spectral characterization and crystal structure of N-2-hydroxy-4-methoxybenzaldehyde-N'-4-nitrobenzoyl hydrazone and its square planar Cu(II) complex. *Spectrochim., Acta Part A Mol., Biomol., Spectrosc.*, **71**, 1253-1260 (2008).
27. Bayoumi H. A., Alaghaz A. M., Aljahdali M. Cu(II), Ni(II), Co(II) and Cr(III) complexes with N<sub>2</sub>O<sub>2</sub>-chelating Schiff's base ligand incorporating azo and sulfonamide moieties: Spectroscopic, electrochemical behavior and thermal decomposition studies. *Int., J., Electrochem., Sci.*, **8**, 9399-9413 (2013).
28. Glu M. K, Ispir E., Glu N. K, Serin S. Novel vic-dioximes: Synthesis, complexation with transition metal ions, spectral studies and biological activity. *Dyes Pigm.*, **77**, 75-80 (2008).
29. Oon Han H., Kim S. H., Kim K. H., Hur G. C., Joo Yim H., Chung H. K., Ho Woo S., Dong Koo K., Lee C. S., Sung Koh J., Kim G. T. Design and synthesis of oxime ethers of  $\alpha$ -acyl- $\beta$ -phenylpropanoic acids as PPAR dual agonists. *Bioorg., Med. Chem., Lett.* **17**, 937-941 (2007).
30. Geary W.J. The use of conductivity measurements in organic solvents for the characterisation of coordination compounds. *Coord., Chem., Rev.*, **7**, 81-122 (1971).
31. Greenwood N. N., Straughan B. P., Wilson A. E. Behaviour of tellurium(IV) chloride, bromide, and iodide in organic solvents and the structures of the species present. *J., Chem., Soc., A: Inorg., Phys., Theo.*, 2209-2212 (1968).
32. Xu G. C., Zhang L., Liu L., Liu G. F., Jia D. Z. Syntheses, characterization and crystal structures of mixed-ligand Cu(II), Ni(II) and Mn(II) complexes of N-(1-phenyl-3-methyl-4-propenylidene-5-

- pyrazolone)-salicylidene hydrazide containing ethanol or pyridine as a coligand. *Polyhedron*, **27**, 12-24 (2008).
33. Samanta B., Chakraborty J., Shit S., Batten S.R., Jensen P., Masuda J .D., Mitre S. Synthesis, characterisation and crystal structures of a few coordination complexes of nickel(II), cobalt(III) and zinc(II) with N'-[(2-pyridyl)methylene] salicyloylhydrazone Schiff base. *Inorg., Chim., Acta*, **360**, 2471-2484 (2007).
  34. Bhosale J. D., Shirolkar A. R., Pete U.D., Zade C.M., Mahajan D.P., Hadole C. D., Pawar S .D., Patil U. D., Dabur R., Bendre R. S. Synthesis, characterization and biological activities of novel substituted formazans of 3,4-dimethyl-1Hpyrrole-2-carbohydrazide derivatives. *J., Pharm., Res.*, **7**, 582-587 (2013).
  35. Singh B. and Srivastava P. Studies on 2,6-diacetylpyridine bis(2-furoylhydrazone) complexes of bivalent 3d-metal ions. *Tran., Met., Chem.*, **12**, 475-477 (1987).
  36. El-Wahab Z.H.A., Mashaly M. M., Salman A. A., El-Shetary B. A., Faheim A.A. Co(II), Ce(III) and UO<sub>2</sub>(VI) bis-salicylatiothiosemicarbazide complexes: Binary and ternary complexes, thermal studies and antimicrobial activity. *Spectrochim. Acta Part A Mol.Biomol. Spectrosc.* **60**, 2861-2873 (2004).
  37. Nakamoto K. Infrared and Raman spectra of inorganic and coordination compounds, 3rd Ed. John Wiley sons, New York, PP. 244 (1977).
  38. Chandra S. Gupta L.K. Spectroscopic studies on Co(II), Ni(II) and Cu(II) complexes with a new macrocyclic ligand: 2,9-dipropyl-3,10-dimethyl-1,4,8,11-tetraaza-5,7:12,14-dibenzocyclotetradeca-1,3,8,10-tetraene. *Spectrochim., Acta Part A Mol., Biomol., Spectrosc.*, **61**, 1181-1188 (2005).
  39. Nakamoto K. Infrared and Raman Spectra of Inorganic and Coordination Compounds, Applications in Coordination, Organometallic, and Bioinorganic Chemistry. 6th ed., John Wiley and Sons: New York; part B, PP. 154 (2009).
  40. Gupta L.K., Bansal U., Chandra S. Spectroscopic and physicochemical studies on nickel(II) complexes of isatin-3,2'-quinolyhydrazones and their adducts. *Spectrochim., Acta Part A Mol. Biomol., Spectro.*, **66**, 972-975 (2007).
  41. Shinde D.B. Synthesis, antileishmanial activity and docking study of N'-substitutedbenzylidene-2-(6,7-dihydrothieno[3,2-c]pyridin-5(4H)-yl) acetohydrazides. *Bioorg., Med., Chem., Lett.*, **24**, 1605-1610 (2014).
  42. EL-Tabl A. S., EL-Saied F. and AL-Hakimi A. N. Spectroscopic characterization and biological activity of metal complexes with an ONO trifunctionalized hydrazone ligand. *J. of Coord., Chem.*, **61**, No. **15**, 2380-2401 (2008).
  43. El-Saied F.A., Al-Hakimi A.N., Wahba M. A. and Shakdofa M. M. Preparation, Characterization and Antimicrobial Activities of N'-((3-(hydroxyimino)butan-2-ylidene)-2 (phenylamino) acetohydrazide and Its Metal Complexes. *Egypt., J. Chem.*, **60**, No. **1**, 1- 24 (2017).
  44. Walaa H. M., Reem G. D. and Gehad G. M. Novel Schiff base ligand and its metal complexes with some transition elements. Synthesis, spectroscopic, thermal analysis, antimicrobial and *in vitro* anticancer activity *Appl., Organo., Chem.*, **30**, 221-230 (2016).
  45. EL-Saied F. A., Shakdofa M. M. E., Al-Hakimi A. N. Synthesis, Characterization and antimicrobial activities of hydrazone ligands derived from 2-(phenylamino)acetohydrazide and their metal complexes. *J., of the Korean Chem., Soci.*, Vol. **55**, No. **3**, 444-453. (2011).
  46. Al-Hakimi A. N., Shakdofa M. Alkwilni A. M., Al Asbahi S. O. Elsaied F. Wahba M. Synthesis, Spectroscopic Characterization and Antimicrobial Activity of Novel Azo-acetohydrazide Metal Complexes *J., Nat., Sci., Math.*, Vol. **10**, No. **1**, 1-26 (2017).
  47. Fouda M. F.R., Abd-Elzaher M. M., Shakdofa M. M., El-Saied F.A., Ayad M. I., El Tabl A. S. Synthesis and characterization of a hydrazone ligand containing antipyrine and its transition metal complexes. *J., Coord., Chem.*, **61**, 1983-1996 (2008).
  48. Parihari R.K., Patel, R. K., Patel R. N. Synthesis and characterization of metal complexes of manganese-, cobalt- and zinc(II) with Schiff base and some neutral ligand. *J., Indian Chem., Soc.*, **77**, 339-340 (2000).
  49. Tiliakos M., Cordopatis P., Terzis A., P. Raptopoulou C., Perlepes S.P. and Manessi-Zoupa E. Reactions of 3d-metal nitrates with N,N'-bis(2-pyridyl)urea (LH<sub>2</sub>): Preparation, X-ray crystal structures and spectroscopic studies of the products trans-[M(II)(ONO<sub>2</sub>)<sub>2</sub>(LH<sub>2</sub>)<sub>2</sub>] (M= Mn, Fe, Co, Ni, Cu, Zn) and mer-[Co(III)(LH<sub>2</sub>)<sub>2</sub>](NO<sub>3</sub>)-MeOH. *Polyhedron*, **20**, 2203-2214 (2001).

50. Wang C.C. Refinement of the crystal structure of aquabis(2,2'-bipyridine)- bis(terephthalato) dicopper(II),  $\text{Cu}_2(\text{H}_2\text{O}) (\text{C}_{10}\text{H}_8\text{N}^2)_2(\text{C}_8\text{H}_4\text{O}_4)_2$ . *Z. Kristallograph. New Cryst., Struct.*, **221**, 385-387 (2006).
51. EL-Tabl A. S., EL-Saied. F. and AL-Hakimi A. N. Synthesis, spectroscopic investigation and biological activity of metal complexes with ONO trifunctionalized hydrazone ligand. *Tran., Met., Chem.*, **701** 32:689- (2007)
52. El-Tabl . A. S., Abd El-Waheed M. M., Wahba M. A., and Abou El-Fadl N. A. Synthesis, Characterization, and Anticancer Activity of New Metal Complexes Derived from 2-Hydroxy-3-(hydroxyimino)-4-oxopentan-2-ylidene benzohydrazide. *Bio., Chem., and Applic.*, Volume 2015, 1-14 (2015).
53. Franklin T. J., Snow G.A. *Biochemistry of Antimicrobial Action*, 4th ed., Chapman and Hall: London, pp 216 (1989).